Power Management Modelling of a Photovoltaic System for a Wireless Sensor Network

Ahmed Shaltout, Petros Spachos, Stefano Gregori
School of Engineering, University of Guelph
Guelph, Ontario, Canada, N1G 2W1
Email: {ashaltou, petros, sgregori}@uoguelph.ca

***Abstract*—In this paper, a power management model for extending the lifetime of a wireless sensor is introduced. The proposed model allows using both the battery and the solar panel to power the sensor. It also shows the limitations of a given system in terms of available and consumed power. An approximate equation for solar irradiation and normalized power is used for quickly assessing the power improvement of the system and can be normalized to the maximum power of any given solar panel. The model then calculates the power thresholds based on the given specifications of the battery, the solar panel, and the power converters. In addition, the model takes the different minimum efficiencies into consideration. The model can further be used to choose component specifications and set power thresholds.**

I. Introduction

Over the past two decades, photovoltaics has expanded along with the growing interest of using renewable alternative energy sources [1]. Photovoltaics has attracted many applications to make use of the sun as a clean energy source to completely power or supplement their main energy source. For most outdoor applications, harvesting energy from the sun is one of the most effective power sources. A prominent application that can use photovoltaics is environmental monitoring. Traditionally, both analog and digital mechanisms were used for measuring physical environmental parameters. Most of those mechanisms required frequent human intervention and had limited monitoring capabilities [2]. Recent advances in low-power wireless network technology made it possible to create small, cost-effective, and smart sensor devices which can measure, record, and communicate environmental data. Wireless Sensor Networks (WSNs) employ a large number of sensors and usually consist of a power supply, a storage unit, a transceiver, a processing unit, and multiple sensors. WSNs have been showing success in a multitude of applications. Several types of sensors can be integrated into a wireless node for different monitoring tasks such as: environmental monitoring [3], structural monitoring [4], [5], and surveillance monitoring [6]. The two main objectives of wireless sensors are to be energy-efficient and cost-effective.

Energy consumption is a primary concern in the design of a WSN, because sensor nodes are usually powered by batteries. The main challenge comes from having to recharge or replace those batteries, especially for WSNs with many nodes. Exploiting the possibility of harvesting solar energy offers an opportunity to achieve extended lifetime for a wireless network. Solar panels can be utilized not only to recharge the batteries but also powering the sensors when possible, therefore maximizing the lifetime of the network. A wireless network should operate unattended for long periods hence, a model should extend network lifetime [7].

For a battery to be charged, the solar panel is required to be at a minimum power level in order for a reversible chemical reaction to occur. The cells in a battery transfer ions from the positive electrode to the negative electrode during charging. However, there is a range of power levels where the energy that the solar panel supplies is not enough to recharge the battery, but still sufficient to power the sensor, this power range is typically not used. In addition, a power management model for optimizing the energy consumption for a given system while avoiding the oversizing of a solar panel can be improved.

In this paper, we present a power management model for extending the lifetime of a wireless node, and minimizing the solar panel size, hence, the overall cost of the network. The paper is organized as follows: in Section II, the physics of the solar cell is briefly discussed with the main differences between a solar cell and a battery highlighted. Section III presents solar irradiance and provides a simple equation that represents irradiation based on spherical trigonometry and compares it to the measured data. Section IV proposes a model for energy optimization based on the output power level of the solar panel. In Section V a practical design example is provided to show the energy optimization model applied to an existing system. Finally, Section VI concludes this work.

II. Power Management Module

The main components of wireless node are: the solar panel, the rechargeable battery, and the sensor node. A solar panel is used to harvest the solar irradiance and uses the photovoltaic effect to convert it into electrical energy. The battery receives the power of the solar panel to get charged, and delivers power to the sensor node as it gets discharged.

A. Solar Cell

A solar cell is the basic building block of a solar panel. The cell is a two terminal device which acts as a diode in the dark and generates a photo-voltage when illuminated by the sun. A single cell can generate between 0 V and 1 V in open circuit and tens of milliamperes when illuminated by the sun. This voltage is low for most applications and hence solar cells are connected in series and in parallel and packaged into a panel

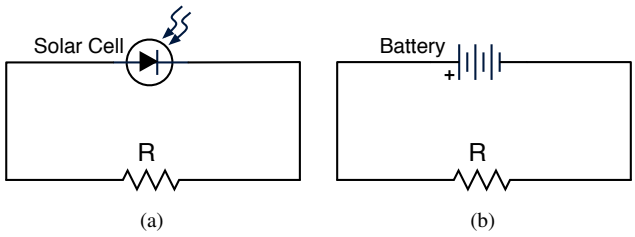

Fig. 1: A solar cell versus a battery in a simple circuit: (a) Solar cell, (b) Battery.

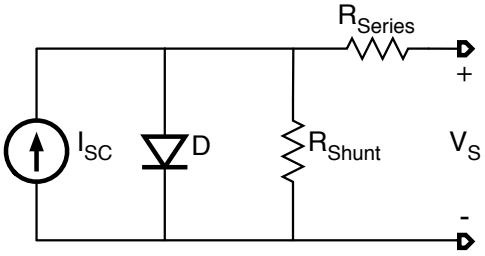

Fig. 2: Equivalent circuit of a solar cell.

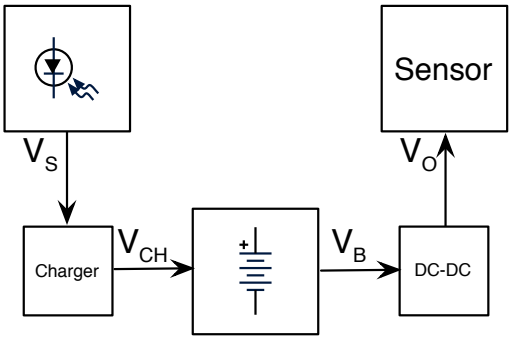

Fig. 3: A simplified block diagram of a common wireless sensor node powered by a rechargeable battery charged by a solar panel.

to produce sufficient output power. The solar cell can replace a battery in a circuit as shown in Fig. 1(a). In the dark, the solar cell does not provide any current, while when the cell is exposed to light, it produces a voltage similar to that of the battery powered circuit in Fig. 1(b). The voltage produced when the terminals of the solar cell are open (R=∞) is the open circuit voltage V_{OC}, which is the highest voltage the cell can produce (usually between 0.5 and 1 V for a single cell [1]). The highest current that can be drawn from the cell when connecting both its terminals together is the short-circuit current I_{SC}. For any load resistance R connected between the terminals of a solar cell, a voltage V is produced that ranges between 0 V at R = 0Ω and V_{OC} at R = $\infty\Omega$, and a current I is delivered to the load such that $V = IR$. The I-V characteristics are determined by the relationship between the current and voltage under given irradiation conditions. Therefore, both V and I are not only determined by the load as in the circuit of Fig. 1(b) but also by irradiation. The current is proportional to the irradiated area, the short-circuit current density is a useful figure of merit. Although the voltage of a simple battery depends on an electrochemical potential difference between the two electrodes, a solar cell derives its voltage from a change in electrochemical potential caused by irradiation. Additionally, the power delivered by a battery is fairly constant for a constant load, while the power delivered by a solar cell depends primarily on the irradiation not the load.

A solar cell can be represented by a current source, in parallel to a diode D and a shunt resistance R_{Shunt} and in series with a series resistance R_{Series} as shown in Fig. 2. The shunt resistance represents the leakage current through the cell around the edges and between contacts, while the series resistance represents the cell material's resistance to the current flow. When the cell is irradiated, it generates a photo-current proportional to the light intensity, that current is divided between the variable resistance of the diode and the load, the ratio of which depends on the level of illumination and the resistance of the load. For higher loads most of the photo-current flows through the diode resulting in a higher voltage across the cell and lower current to the load.

B. System Description

A simplified block diagram of a typical power management of a wireless node is shown in Fig. 3. The conventional power management of a wireless node functions as follows: the solar panel charges the battery through a battery charger block, and the battery discharges to the sensor after being conditioned using a boost dc-dc converter. The battery charger sets a threshold voltage V_{CH} and current I_{CH} for the solar panel in order to charge the battery. In certain lighting conditions, the output power of the solar panel is large enough to enable the battery charger, which initiates the charging cycle. The battery charger checks the voltage level of the battery, if it is completely depleted the charger enters a "pre-charge" phase in which the current supplied to the battery is gradually increased while the battery's voltage is monitored until it reaches a level at which a higher constant current can be supplied to charge the battery. Usually, there is a termination voltage for the battery at which the voltage supplied to the battery becomes constant while the current supplied is monitored to determine when the battery is fully charged.

Depending on the size of the rechargeable battery, both thresholds V_{CH} and I_{CH} are determined. Therefore, even if the sensor is operating during the day with light intensity that is not high enough to enable the charger then, the sensor module would fail to operate, unless the battery is still charged. A typical situation is shown in Fig. 4, where the solid black line represents a typical minimum output power that is required to charge the battery. The dotted curve represents the average calculated irradiation in June, while the dashed curve represents the average irradiation in December, both in Toronto. As shown by the black line the powers higher than

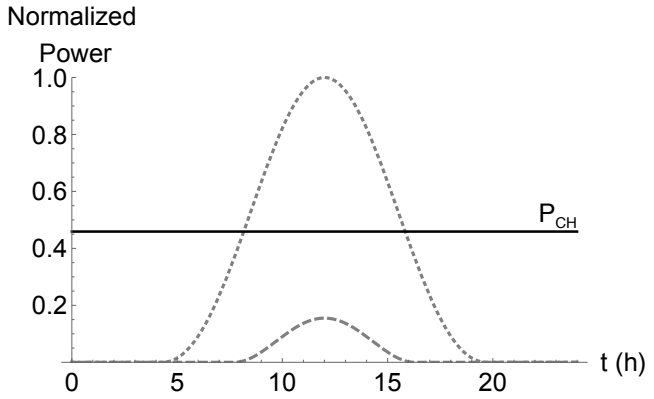

Fig. 4: The normalized power per hour of day for June (dotted) and December (dashed), the solid black line shows a typical minimum power required to charge the battery.

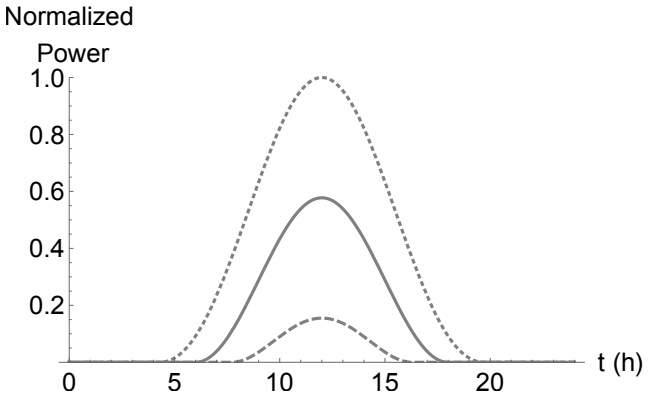

Fig. 5: The normalized power per hour of day for the months of June (dotted), September/ March (solid), and December (dashed).

this threshold are wasted and the powers lower are not used. The main objective is to be able to use the range of powers below the minimum required by the battery and to optimize the size of the solar panel so that the wasted range is minimized.

III. Solar Irradiance

The distribution of the total solar irradiance on the Earth's surface and can apply to any beam incident to a rotating sphere. The irradiation E_e is based on a basic identity from spherical trigonometry [8]. The total irradiance can be written as

$$E_e \propto (\sin\phi \sin\delta + \cos\phi \cos\delta \cos\tfrac{\pi}{12}(t-12))^2. \quad (1)$$

where ϕ is the latitude (location of solar panel), δ is the axial tilt of the Earth which ranges between $-23.5°$ ($-0.131\,\pi$) in December's solstice to $23.5°$ ($0.131\,\pi$) in June's solstice, and t is the time of the day in hours (0 to 24). The maximum irradiation in a given location $E_{e,max}$ is given by

$$E_{e,max} \propto (\sin\phi \sin\delta_0 + \cos\phi \cos\delta_0)^2. \quad (2)$$

where $\delta_0 = 0.131\ \pi$ is δ at the June solstice. The irradiance equation is normalized by dividing it by the maximum irradiance and is expressed as

$$P_n = E_{e,n} \propto \frac{E_e}{E_{e,max}} = \frac{(\sin\phi \sin\delta + \cos\phi \cos\delta \cos\tfrac{\pi}{12}(t-12))^2}{(\sin\phi \sin\delta_0 + \cos\phi \cos\delta_0)^2}. \quad (3)$$

The latitude ϕ is set constant to Toronto's latitude of 43.7°, while a parametric sweep is being performed on δ from $-\delta_0$ to δ_0 and t from 0 to 24 h. The average power produced by a solar panel with fixed orientation (without obstructions) has the same simplified expression ($E_{e,n} = P_n$). Fig. 5 shows the normalized total solar irradiance throughout the day. The two limit cases of $\delta = -\delta_0$ (dashed line) representing December's solstice and $\delta = \delta_0$ (dotted line) representing June's solstice show the minimum and maximum irradiation, respectively.

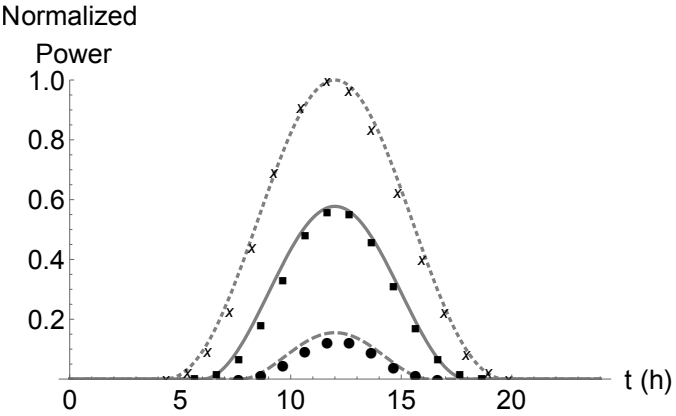

Fig. 6: The normalized power per hour of day for the months of June (dotted) calculated and (x) measured, September/ March (solid) calculated and (■) measured, and December (dashed) calculated and (•) measured.

The third average case is when $\delta = 0$ which represents September's/ March's equinox (solid line).

The measured data available from Environment Canada [9] for the normalized UV-Index in different months averaged for the years 1989 to 2001 is in good agreement with the irradiance equation curves as shown in Fig. 6. The equation for June is represented by the dotted curve, while the data measured by Environment Canada for June is normalized and represented by 'x'. For September/ March the equation is represented by the solid curve and the data by 'square'. December equation is represented by the dashed curve while the data is symbolized by 'circle'.

IV. Energy optimization

As mentioned previously the power range below the battery's threshold cannot be used by the system since it is not adequate to power the battery. A modified block diagram is shown in Fig. 7 where both the solar panel and the battery control a PMU. The main components of the PMU are a

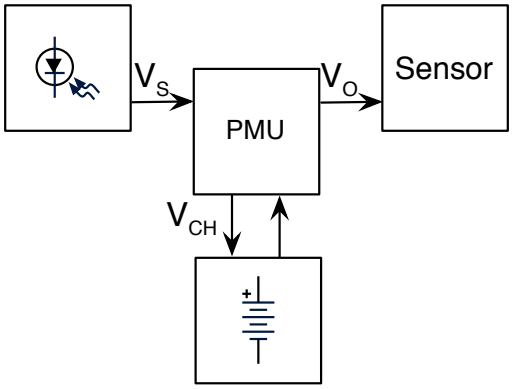

Fig. 7: The proposed simplified block diagram of the system.

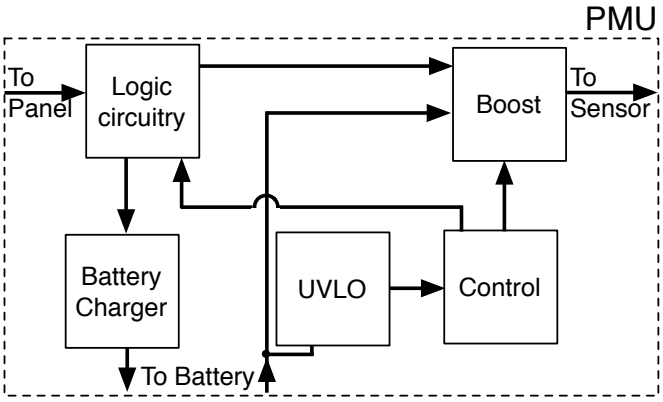

Fig. 8: The proposed simplified block diagram of the PMU.

battery charging block, a boost converter block, and an under-voltage lockout block. The main idea is to be able to use the lower range of power that is adequate to supply the sensor.

A. System Operation

For simplicity, the sensor is assumed to have only two operation modes. The sensor draws a certain amount of current I_{OUT} at a certain voltage level V_{OUT}. A block diagram of the PMU is shown in Fig. 8. The solar panel is connected to a logic circuitry that senses both the current and voltage levels of the solar panel and then decides to connect the panel to the battery charger, the boost converter, or completely disable it. In the first case, the output power of the solar panel, P_S should be at least equal to the battery's charging threshold. In the proposed second case, the output power of the solar panel is less than the charging threshold but greater than the boost converter's threshold, P_B. In the last case the solar power is lower than P_B and the solar panel is disabled.

In the first case when, $P_S \geq P_{CH}$, the system behaves similarly to the conventional system. The battery charger senses the voltage and current of the battery and determines which charging mode to select accordingly. The charger uses maximum power point tracking to maximize the power output of the solar panel. Additionally, a buck converter can be integrated into the battery charger in order to make full use of the range of output voltages from the solar panel. Panel voltages higher than the charging voltage of the battery should be stepped down to the charging voltage which will step up the charging current, I_{CH}, that is essential for both optimally using the available energy and speeding up the charging process.

The battery is also connected to an under-voltage lockout block that sets a lower bound to the battery's voltage at which is sends a signal to the control block to disable the boost block (i.e. disable the whole system). Alternatively, the control block can send the logic circuitry a signal to check if the solar power is sufficient to power the boost converter.

The second case starts when $P_B \leq P_S \leq P_{CH}$, where P_B is the minimum power required to operate the boost converter. The task of the boost converter is to step up its input voltage to a higher level while still providing a sufficient current to power the sensor. Assume that the boost converter's input voltage is V_{IN} and the input current is I_{IN}, resulting in an input power of P_{IN}. The boost converter is not ideal and hence there are some internal power losses associated mainly with the inductor and the switches given by P_{LOSS}. The amount of losses defines the efficiency of a given converter

$$\eta = \frac{P_{OUT}}{P_{IN}} = \frac{P_{OUT}}{P_{OUT} + P_{LOSS}}. \tag{4}$$

In order to be able to drive the boost converter, P_{IN} has to be larger than P_{OUT}. In addition, a boost converter has a certain line regulation and so it can tolerate a range of input voltages while producing the same output voltage, however, this comes with a cost in reduced efficiency as the input voltage decreases further. Therefore, the P_B threshold should be chosen so that V_B is the minimum voltage the boost converter can operate on and I_B is high enough so that the product accommodates the required P_{OUT} and P_{LOSS}

$$I_{IN} = \frac{\eta_{min}(P_{OUT} + P_{LOSS,max})}{V_{IN,min}}, \tag{5}$$

where η_{min} is the minimum efficiency of the boost converter at a given load current and output voltage, where V_{IN} is the lowest allowed by the boost converter $V_{IN,min}$.

To further clarify the different cases, Fig. 9 shows the normalized power per hour of day, for June and December in dotted and dashed curves, respectively. The minimum power required for charging the battery, P_{CH}, is represented by the solid line and the minimum power required for operating the boost converter, P_B, is represented by the dot-dashed line.

V. Design Example

The wireless nodes in this work are based on the same structure of [10] and [11]. The hardware components of the system are: a control node, a sensor node, and a solar module. The control node is the base of the network as it collects the data from all the different sensor nodes. It allows bidirectional communication to access data form the sensor and also sends commands to the nodes. However, the control node is not the main concern of this work as there is usually one or just a

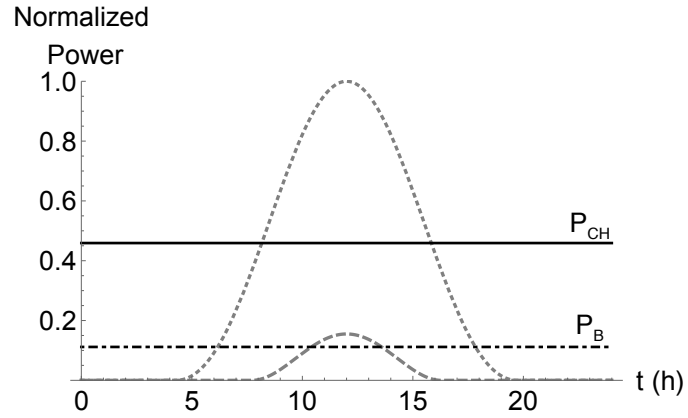

Fig. 9: The normalized power per hour of day for June (dotted) and December (dashed), the solid black line shows a typical minimum power required to charge the battery and the proposed threshold (dot-dashed) represents the minimum usable power to operate the sensor.

few control nodes and power consumption is not the main constraint for them.

The sensor node is considered the load of the proposed PMU, in this design example the sensor device is a DHT11 temperature and humidity sensor which is connected to a radio module by a single-wire interface which provides digital temperature and humidity readings. The data from the sensor is read at intervals, formatted into packets, and transferred to the radio module for scheduling and transmission. The radio module is an OMesh Networks RapidMesh OPM15 Development Board [12]. The module consists of a micro-controller, two antennas, and a radio chip. The radio module executes spectrum sensing and transmits the sensed data. Additionally, it can implement routing protocols to further improve the energy efficiency [10].

The solar module is the power supply of the sensor nodes. Each solar module consists of a solar panel, a rechargeable battery, and a PMU. The solar panel used is a commercial 12-cell, 165 mm×165 mm solar panel (4.5 W, 720 mA, 7.2 V). The rechargeable battery is a 3.7 V lithium-ion polymer battery rated at 6600 mAh. The panel and the battery are connected via the PMU as shown in Fig. 3. The original system was optimized to be as small as possible to cause minimum interference to the environment and the battery was chosen to be able to supply continuous power to the node for 48 hours without sun. Depending on the application, a network's lifetime can be defined [7]. In this paper, the lifetimes is defined as the time it takes a node until connectivity is lost between the source and the destination. Network survivability is essential and this is where the model developed in the previous section becomes effective.

The first power threshold, P_{CH}, is calculated as follows: first, assume the battery capacity is C, the efficiency of charging is η_{CH}, and the time to fully charge the battery is t_{CH}. The current required to charge the battery is given by I_{CH} is given by

$$I_{CH} = \frac{C + C(1 - \eta_{CH})}{t_{CH}} = \frac{C(2 - \eta_{CH})}{t_{CH}}. \quad (6)$$

The charging current, I_{CH}, has to always be lower than the maximum charge current which is always the case in WSNs. Since every battery has a given constant charging voltage, V_{CH}, the minimum power required to charge the battery, P_{CH} is then given by $I_{CH} \times V_{CH}$. In this design example t_{CH} was set to 13 h, which is the average number of hours of light over the year based on the data from Environment Canada [9]. The efficiency, η_{CH}, is 0.8, for which I_{CH} is calculated from (6) to be 609 mA. At V_{CH} of 4.2 V the minimum power is 2.56 W. For voltages higher than 4.2 V the buck converter in the battery charger will step them down to the charging voltage which will step up the current, in the limit case of 7.2 V, by 1.7 times.

The second power threshold, P_B, is determined by both the efficiency of the boost converter at the input voltage V_{IN} range and the load current, I_{OUT}, and output voltage, V_{OUT}, which are determined by the sensor module. The sensor module used requires 65 mA at 5 V to operate so the output power of the boost converter should be 325 mW. However, in this example the boost converter can accept, V_{IN}, from 1 V to 4 V to be boosted to 5 V, the efficiency of the converter, η_B, is variable for a constant output power based on the exact input voltage. In the worst case, the boost converter will be required to step up a 1 V to 5 V, with a typical efficiency, η_B, of about 0.7. The power loss in this case is 139.3 mW and the input power is 465 mW. From (5), the minimum input current, I_{IN}, required is calculated to be 465 mA.

The relative power in (3) is then normalized to the maximum power and solved for both power thresholds. Fig. 10 shows the power in watt versus the time of the day for the month of June as one limit case, the charging threshold is a solid horizontal line while the boost threshold is a dot-dashed line. The figure highlights four different regions: A, B, C, and D. In the conventional model [10] only regions A and B are applicable. In region A, the solar panel can provide adequate power to charge the battery, at the same time the battery is required to power on the sensor. In region B, the power provided by the solar panel is not sufficient to charge the battery, so the battery has to supply the sensor until it is depleted. Region A is about 6 h (09:01 to 14:59) which will charge a depleted battery to about half capacity. The battery should then supply the sensor until the around 09:01 the next day, assuming good.

In the proposed model, there are 3 regions: A, C, and D. Region A is identical to the conventional model. In region D the system behaves exactly like the conventional system except for a shortened period. In region C, the solar panel is used solely to power the sensor as explained, which is divided into two regions one from (06:13 to 9:01) and the second from (14:59 to 17:47) which relieves the battery from being used for an extra 05 h 38 min, which achieves a saving in the energy stored in the battery by 23.4%. The system can be further optimized by allowing the solar panel to supply

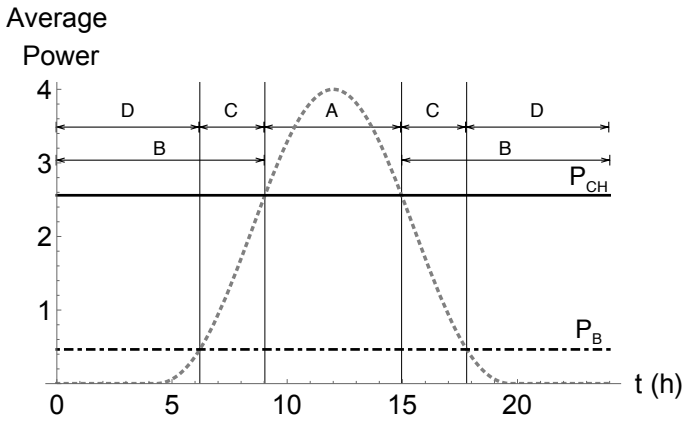

Fig. 10: The power per hour of day for June (dotted), the solid black line shows the minimum power required to charge the battery (2.56 W) and the proposed threshold (dot-dashed) represents the minimum usable power to operate the sensor (0.465 W), the different regions of the day are highlighted.

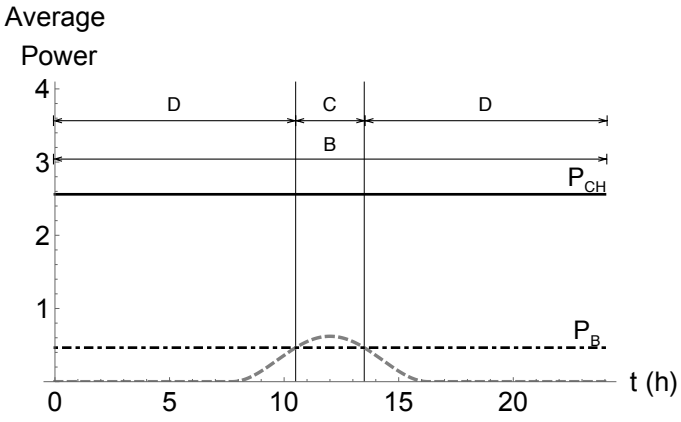

Fig. 11: The power per hour of day for December (dashed), the solid black line shows the minimum power required to charge the battery (2.56 W) and the proposed threshold (dot-dashed) represents the minimum usable power to operate the sensor (0.465 W), the different regions of the day are highlighted.

the sensor at the time the battery is being charged, therefore, saving the battery from having to supply the system for an extra 6 h which saves the stored energy by 48.8%.

The other limit case is for the month of December shown in Fig. 11 where the power is in watt. As shown in the figure, region A is non existent and the system is always in region B, which means that for the conventional model the node would either completely disconnect or a manual intervention would be required, where the battery would be charged or replaced. For the proposed model, the sensor can still be powered in region C by the solar panel without the need for the battery, for almost 3 h from (10:30 to 13:30). For some systems it is sufficient to have the sensor take readings only a few times per day for which the proposed model is effective and no human intervention is necessary. If the system is to work for more hours, then the solar cell used has to be larger by 5 times for the proposed model, while for the conventional model it would have to be 7 times larger for the system to work the same number of hours. This provides an area saving of 28.5%.

VI. Conclusion

In this paper, a power management model for a wireless sensor was introduced. The model makes minor modifications to the power management unit by simply bypassing the battery charger when the illumination conditions are not sufficient for the solar panel to generate enough power to charge the battery. The proposed model was then applied to an existing configuration to calculate the percentage of energy saving for the two limit cases of June and December. The model can be easily adapted to make different component selections. Using this model, the battery lifetime can be extended since it will go through less full charge/discharge cycles for the same period of time compared to the original system which will in turn extend the life time of the wireless sensor network. The next steps are to deploy the network in an environment, evaluate the improvement in power consumption in comparison to the original model, and determine if any changes are needed to further improve the performance.

References

[1] J. Nelson, *The Physics of Solar Cells*, 1st ed. London, England: Imperial College Press, 2003.

[2] L. Oliveira, J. Rodrigues, "Wireless Sensor Networks: a Survey on Environmental Monitoring," *J. Commun.*, vol. 6, no. 2, pp. 143–151, Apr. 2011.

[3] O. A. Postolache, J. M. D. Pereira, and P. M. B. S. Girao, "Smart Sensors Network for Air Quality Monitoring Applications," *IEEE Trans. Instrum. Meas.*, vol. 58, no. 9, pp. 3253–3262, Sep. 2009.

[4] T. Torfs, T. Sterken, S. Brebels, J. Santana, R. van den Hoven, V. Spiering, N. Bertsch, D. Trapani, and D. Zonta, "Low Power Wireless Sensor Network for Building Monitoring," *IEEE Sensors J.*, vol. 13, no. 3, pp. 909–915, Mar. 2013.

[5] E. Sazonov, H. Li, D. Curry, and P. Pillay, "Self-Powered Sensors for Monitoring of Highway Bridges," *IEEE Sensors J.*, vol. 9, no. 11, pp. 1422–1429, Nov. 2009.

[6] D. S. Ghataoura, J. E. Mitchell, and G. E. Matich, "Networking and Application Interface Technology for Wireless Sensor Network Surveillance and Monitoring," *IEEE Commun. Mag.*, vol. 49, no. 10, pp. 90–97, Oct. 2011.

[7] I. Dietrich and F. Dressler, "On the Lifetime of Wireless Sensor Networks," *ACM Trans. Sensor Netw.*, vol. 5, no. 1, pp. 1–39, Feb. 2009.

[8] I. Todhunter, *Spherical Trigonometry*, 5th ed. London, England: Macmillan and Co., 2006.

[9] (2002, Jan.) Environment Canada Ozone and UV Monitoring. [Online]. Available: http://exp-studies.tor.ec.gc.ca/

[10] P. Spachos and D. Hatzinakos, "Self-Powered Wireless Sensor Network for Environmental Monitoring," in *Proc. IEEE Globecom Workshop,* San Diego, CA, Dec. 2015, pp. 1–6.

[11] P. Spachos, L. Song, and D. Hatzinakos, "Prototypes of Opportunistic Wireless Sensor Networks Supporting Indoor Air Quality Monitoring," in *Proc. IEEE Consumer Commun. Netw. Conf.,* Las Vegas, NV, Jan. 2013, pp. 851–852.

[12] (2011, Aug.) OMESH Networks - OPM15. [Online]. Available: http://www.omeshnet.com/omesh/